Molecular Shape and Intermolecular Liaison: Hydrocarbons and Fluorocarbons

by **Jack D. Dunitz***[a]), **Angelo Gavezzotti***[b]), and **W. Bernd Schweizer***[a])

[a]) Organic Chemistry Laboratory, Swiss Federal Institute of Technology, ETH-Hönggerberg, CH-8093 Zürich
[b]) Dipartimento di Chimica Strutturale e Stereochimica Inorganica, Università di Milano, I-20133 Milano

'*What though youth gave love and roses,*
Age still leaves us friends and wine.'

Thomas Moore, 'Spring and Autumn'

For *Duilio*, at seventyfive

Whereas aliphatic hydrocarbon/fluorocarbon mixtures show mutual 'phobicity' (*e.g.*, positive deviations from *Raoult*'s Law), their aromatic counterparts show the opposite behavior. Hexafluorobenzene forms co-crystals with many aromatic hydrocarbons, but co-crystals are unknown in the aliphatic series. This remarkable contrast between the behaviors of aliphatic and aromatic hydrocarbon/fluorocarbon mixtures calls for explanation, and we attempt to provide one in terms of the difference in overall molecular shape – disk *vs.* cylinder – using the new PIXEL method for calculating intermolecular energies.

Introduction. – The mutual phobicity of aliphatic hydrocarbons and fluorocarbons has been recognized as a remarkable phenomenon ever since the latter compounds became available. As noted in the classic monograph '*Regular and Related Solutions*' [1], '*However, before the advent of fluorocarbons, nonpolar components sufficiently unlike to yield two liquid phases were scarce. …The advent of fluorocarbons provided a new set of nonpolar liquids which are only partially miscible with other common, nonpolar liquids*'. As examples of mutual phobicity may be mentioned the high consolute temperatures of C_6F_{14}/C_6H_{14} (296 K) and of c-C_6F_{12}/c-C_6H_{12} (316 K), and the strongly non-ideal behavior of C_4F_{10}/C_4H_{10} at 295.6 K, where the partial vapor pressures of the components are much greater than expected for ideal behavior (*Raoult*'s law). Gas-phase measurements indicate that fluorocarbon–hydrocarbon interaction energies are *ca.* 10% weaker than expected on the basis of fluorocarbon–fluorocarbon and hydrocarbon–hydrocarbon interaction energies [2]. It came then as something of a surprise that, in sharp contrast to the behavior of the aliphatic compounds, hexafluorobenzene was found to form a 1:1 co-crystal with benzene with a higher melting point than either component [3]. Also, in contrast to the behavior of the aliphatic liquid mixtures, solutions of hexafluorobenzene and aromatic hydrocarbons show negative deviations from *Raoult*'s law, *i.e.*, they show mutual attraction of the component molecules rather than mutual phobicity. Since then, dozens of solid compounds of hexafluorobenzene with aromatic hydrocarbons have been isolated and their crystal structures determined. The characteristic feature of these co-crystal structures is that they are built from stacks in which the two kinds of molecule alternate with their planes parallel and separated by *ca.* 3.5 Å. In the aliphatic series, co-crystals

of alkanes and perfluoroalkanes are unknown. These striking differences between the liquid behaviors of aliphatic and aromatic fluorocarbon/hydrocarbon mixtures are thus duplicated in the solid state and must surely depend on the differences in overall molecular shape – disks *vs.* cylinders – and it seems useful to try to express such differences in terms of intermolecular interaction energies. Here, we take up the problem with the help of intermolecular interaction energies obtained by a new method involving direct numerical integration over electron densities [4][5], but first we describe and discuss physical properties of the hydrocarbons, their fluorinated analogs, their mixtures, and their crystal structures in somewhat more detail.

Physical Properties. – One striking feature of the hydrocarbons and their perfluorinated analogs is the similarity of many of their physical properties: boiling points, enthalpies of vaporization, molecular polarizabilities. These similarities may seem surprising in view of the much larger atomic weight and atomic number of F compared with H. However, the additional electrons are tightly bound by the F nuclei, with the result that the atom polarizability of F is close to that of H. For example, from a recent tabulation [6], we find the values 0.41, 0.44, and 1.29 $Å^3$ for the effective atomic polarizabilities of H, F, and C, respectively. Hydrocarbons and their corresponding perfluorocarbons have nearly equal molecular polarizabilities. Of course, the densities of the fluorocarbons are much higher than those of the corresponding hydrocarbons, and so are their molecular volumes, while their surface tensions and refractive indices are lower. These and other similarities and differences are described and discussed in several reviews [7][8][9], but from our point of view it is the similarities in the physical properties between hydrocarbons and their perfluorinated analogs that are the more remarkable. As far as boiling points are concerned, that of CH_4 is some 50° lower than that of CF_4 (195 K), but as chain length in the aliphatic series increases, the difference becomes smaller, falling to zero for C_4H_{10} and C_4F_{10} (both 272 K), while, for longer chain length, it is the perfluorocarbon that has a slightly lower boiling point (*e.g.*, hexane, 342 K; perfluorohexane, 330 K). In the aromatic series, the boiling points of benzene and hexafluorobenzene are practically equal (354 and 355 K resp.), and indeed the boiling points in the whole series of partially fluorinated benzenes vary only within a small range (349 to 367 K). In contrast, the boiling points of the partially fluorinated methanes do differ systematically: CH_4 (112 K), CH_3F (195 K), CH_2F_2 (221 K), CHF_3 (191 K), CF_4 (165 K), a trend that runs parallel to the molecular dipole moments and has been invoked as evidence for C–H···F H-bonding in the liquids. However, if this explanation is accepted, it is difficult to see why the partially fluorinated benzenes should not also show analogous behavior.

Crystal Structures. – During the last few years, crystal structures have been determined for co-crystals of hexafluorobenzene with many aromatic compounds and for crystalline compounds with molecules containing both phenyl and pentafluorophenyl groups. The characteristic of almost all these crystals is the presence of mixed stacks of parallel (or nearly parallel), alternating hydrocarbon and perfluorinated moieties. These structures have been generally interpreted mainly in terms of electrostatic interactions, with models ranging from high-level quantum-mechanical calculations to qualitative considerations based on interactions among molecular

quadrupole moments. We shall discuss some of these in more detail later. The situation for the aliphatic series is less satisfactory. While the crystal structures of the alkanes from propane to decane have recently been determined at low temperatures [10], the only aliphatic perfluorocarbon whose structure is known in the solid state is perfluorohexane [11]. As for the alkanes, from hexane onward, the centrosymmetric even-membered chains pack with all molecules parallel ($P\bar{1}$, $Z=1$) while successive C_2-symmetric odd-membered chains are related by inversion centers ($P\bar{1}$, $Z=2$). There are thus differences between the packing of the terminal Me groups in the even- and odd-membered chains, which account for the well-known melting-point alternation in these compounds [10]. In contrast to the aliphatic C chains with planar zigzag conformation, the perfluorohexane chain is helical with twist angles of *ca.* 13° around each C–C bond. A similar helical structure (twist angle *ca.* 14°) was deduced many years ago for the C chain of poly(tetrafluoroethene) (*Teflon*®) [12][13]. As *Bunn* and *Howells* [12] pointed out, F-atoms attached to a planar zigzag chain would be overcrowded, and the helical structure increases the distance between such F-atoms to more tolerable distances (from *ca.* 2.52 Å in the planar zigzag chain with 110° bond angle to *ca.* 2.7 Å in the helical chain with bond angle widening to *ca.* 116°). Perfluoroalkane chains in some crystal structures are described as being nearly planar, but this is probably the result of thermal disorder involving partial unwinding of the chains. From the many crystal structures of compounds containing fluorinated chains, it is clear that these tend to segregate. A particularly instructive example is the crystal structure of 12,12,13,13,14,14,15,15,16,16,17,17,17-tridecafluoroheptadecan-1-ol [14] (CCDC refcode TULQOG), where the long chain bends at the junction of the two segments in such a way that the shortest intermolecular C···C distances are *ca.* 4 Å between hydrocarbon segments and *ca.* 5 Å between fluorocarbon ones. As in other crystal structures containing hydrocarbon and fluorocarbon segments, the two kinds of chain segregate into quite distinct separate layers (*Fig. 1*).

Fluorobenzenes. The fluorobenzenes form a particularly interesting series. The partially fluorinated compounds have melting points between 225 and 277 K, the higher temperature being almost the same as the melting points of benzene and hexafluorobenzene. As mentioned, the compounds have nearly the same boiling points (349 to 367 K) and molecular polarizabilities (10.2 to 10.7 Å^3). The crystal structures of most of the partially fluorinated benzenes have been determined and discussed in great detail in terms of C–H···F interactions [15]. This emphasis on C–H···F interactions, which are after all unavoidable in this class of compounds, could well have distracted attention from other types of interaction that may be more important in determining the types of crystal structure adopted by these compounds. For example, from the similarity of the fluorobenzene crystal structure to that of pyridinium fluoride (and other compounds), *Thalladi et al.* concluded that the C–H···F interaction is important in the former. However, the fluorobenzene structure is also closely similar to the virtual structure N5 of benzene [16] which has a calculated packing energy only *ca.* 1 kJ · mol^{-1} less than that of the observed benzene structure [17]. Fluorobenzene and N5 benzene have the same space group $P4_12_12$ and similar unit-cell dimensions: $a=b=5.80$ Å, $c=14.53$ Å for fluorobenzene, $a=b=5.54$ Å, $c=15.32$ Å for N5 benzene. Pyridinium fluoride and benzonitrile are also closely isostructural. One might conclude that it is simply the similarity in molecular shape that can lead to similar crystal packings for a great variety

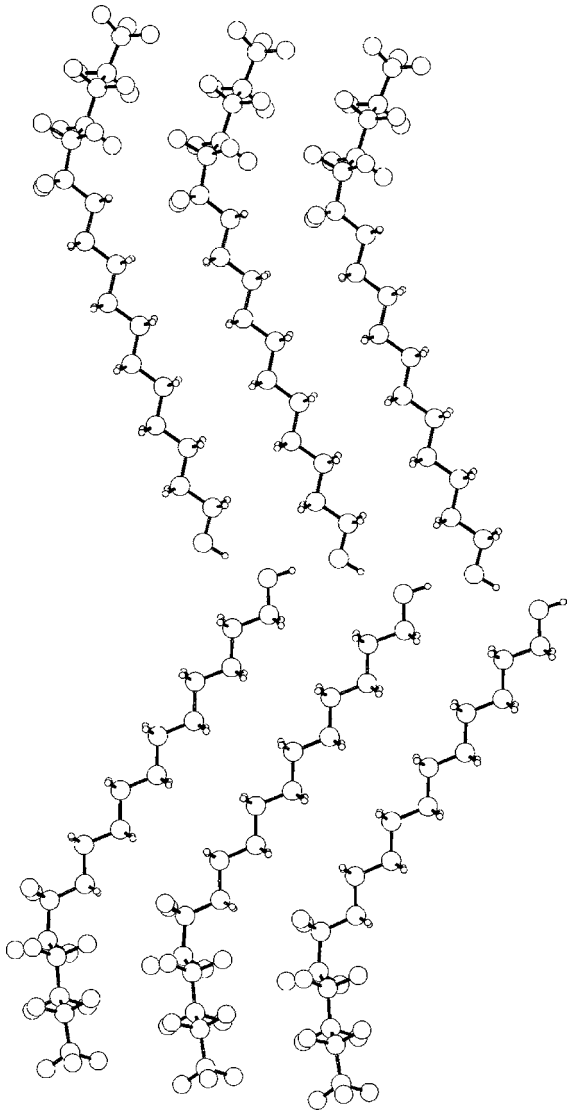

Fig. 1. *Crystal structure of 12,12,13,13,14,14,15,15,16,16,17,17,17-tridecafluoroheptadecan-1-ol* [14] (CCDC refcode TULQOG), *showing segregation of hydrocarbon and fluorocarbon chain segments*

of local intermolecular interactions. Along the same line, the observed crystal structure of 1,4-difluorobenzene, also discussed by *Thalladi et al.* [15] in terms of C–H···F interactions, is closely isostructural with benzene virtual structure N2 with calculated packing energy within 0.3 kJ/mol of that of benzene [16].

Perhaps even more interesting than these similarities is the structure obtained for 1,3,5-trifluorobenzene, described by *Thalladi et al.* [15] with respect to its similarity to that of 1,3,5-triazine and the identical role of C–H···F interactions and C–H···N H-

bonds in these structures. The most-striking feature of the 1,3,5-trifluorobenzene crystal structure is surely the presence of the tightly packed stacks in which alternate molecules are related by inversion centers so as to place the F-atoms of one molecule almost over the H-atoms of its two neighbors in the stack (*Fig. 2*). The distance between the molecular planes in the stacks is 3.51 Å, and the stacks are arranged in quasi-hexagonal packing (with C–H···F interactions between molecules in neighboring stacks). The analogy between this structure and that of the 1:1 benzene/hexafluorobenzene structure [18] can hardly be overlooked. Whereas the molecules of benzene and hexafluorobenzene are complementary as far as their charge distributions are concerned (they have nearly equal quadrupole moments but of opposite sign [19]), the molecules of 1,3,5-tifluorobenzene are self-complementary (and have only a small quadrupole moment [20]). The crystal structure of 1,2,3-trifluorobenzene was not determined by *Thalladi et al.* [15] but, since the same self-complementary property can also be ascribed to this molecule, one might predict that its crystal structure would be very similar to that of the 1,3,5-isomer with the same kind of molecular stacking. A new determination [11] shows that this is indeed the case. Similar stacks, but with larger slip displacements of adjacent molecules, also characterize the crystal structures of 1,2,4,5-tetrafluorobenzene and the *C2/c* polymorph of the 1,2,3,4-isomer. In these stacks, an F-atom of one molecule sits almost over the ring-center of its neighbor, and the distances between the molecular planes are very short – less than 3.4 Å.

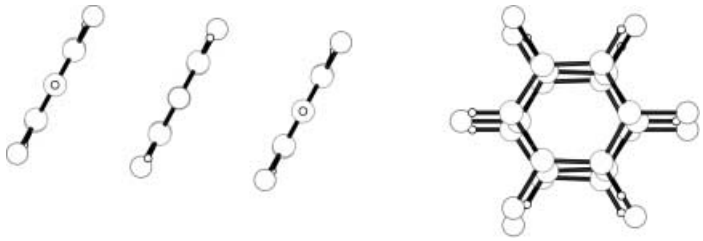

Fig. 2. *Stacking of 1,3,5-trifluorobenzene molecules as observed in the crystal structure* [15]

The other 1,2,3,4-tetrafluorobenzene polymorph ($P2_1/n$) contains centrosymmetric dimers with interplanar distance of 3.62 Å, and these dimers are then packed in a herring-bone arrangement. Finally, as noted by *Thalladi et al.* [15], the pentafluorobenzene crystal structure contains two symmetry-independent molecules, each of which forms a stacked centrosymmetric dimer (interplanar distances 3.58 and 3.62 Å), which is packed in herring-bone fashion. The crystal structure of hexafluorobenzene [21], the end member of the series, also contains two symmetry-independent molecules and a herring-bone type of packing. Thus, the prominent stacks of parallel (or rather anti-parallel) molecules occur only for the tri- and tetrasubstituted molecules, with small slip displacements for the former and large ones for the latter.

Calculations. – The recently developed SCDS (semi-classical density sums, or PIXEL) method [4][5] was designed primarily for calculating lattice energies of crystals, but it is also suited for estimating interaction energies of small molecular clusters, as illustrated in a recent report on the 1:1 acetylene/benzene co-crystal [22].

Here we apply it mainly for estimating the interaction energies of homo- and hetero-dimers of hydrocarbons and fluorocarbons. Since this new method is not yet entirely free of growing pains, we also check its performance by calculating the dimer energies with the well-known UNI force-field, based on empirical *Buckingham*-type atom–atom potentials.

Briefly, the PIXEL calculation of intermolecular energies starts by obtaining the electron density for each molecule by standard quantum-mechanical methods, using a step of 0.08 A for a grid that usually contains *ca.* 10^6 'cube-lets' (original pixels). This density grid is then condensed into $n \times n \times n$ super-cubes ($n = 4$ here), and pixels containing less than 10^{-6} electrons are discarded as insignificant, so that the molecular-density ends up being described by some 10,000 pixels. The positions of all pixels and all nuclei are then repeated in space by selected rotation and translation operations, or by space-group symmetry operations if a crystal is considered. Thus, the method assumes a juxtaposition of rigid, undistorted, electron densities of separated molecules in a supramolecular array. The coulombic energy between any two molecules is calculated simply as a sum over $q_i q_j / r_{ij}$ contributions from each pair of electron-density pixels in the separate molecules. Thus, it does not depend on any assignment of point charges or distributed multipoles at the nuclear positions. At the short distances between adjacent molecules in condensed phases, the coulombic energy calculated by the PIXEL method is much more reliable than that based on electrostatic interactions among any such distribution of point charges and multipoles within the molecules.

The repulsion energy is taken to be proportional to the overlap of the electron densities, which is also calculated by numerical integration, elevated to a power slightly smaller than one. This requires at least two empirical parameters that are not always easy to determine. For the estimation of the polarization energy, each electron-density pixel is allotted to an atom (the one to whose nucleus the distance is the smallest fraction of the atomic radius), and the pixel polarizability is taken as the corresponding atom polarizability (atom polarizabilities and atomic radii used for this purpose are listed in *Table 1*[1]). The polarization energy is then calculated as a many-body effect resulting from the action of the total electric field from all surrounding molecules, at each pixel *via* the induced dipole and the linear polarization formula, summed over all pixels. The dispersion energy is obtained as a sum of pixel-pixel terms by a *London*-type formula, using the pixel polarizabilities and the overall molecular-ionization potential taken as the energy of the highest occupied molecular orbital (HOMO). Polarization and dispersion energies are multiplied by an appropriate damping function to avoid singularities, and this introduces two more empirical parameters. The total interaction energy is then the sum of the coulombic, polarization, dispersion, and repulsion terms. The method uses only four fully disposable parameters and is described in detail in [5][2]).

---

[1]) Although atom polarizabilities are not rigorously definable quantities, experimentally or theoretically determined molecular polarizabilities can be reproduced as sums of self-consistent sets of atom polarizabilities. Various sets are available. Similarly for atomic radii (see *Table 1*).

[2]) Here we use a slight variant of the previous calibration [5], resulting from a further round of adjustments based on a much more-extensive data set: $D = 3.25$ A^{-1}, $\varepsilon_{max} = 170 \times 10^{10}$ V m^{-1}, $K = 3300$, and $\gamma = 0.97$. The polarizability of the aromatic carbon atom was reduced from 1.30 to 1.25 A^3. Full details will be published elsewhere.

Table 1. *Atomic Polarizabilities and Atomic Radii Used in the Calculations*

Atom type	Polarizability [A^3]	Intermolecular radius [Å]
C, aliphatic	1.05	1.77
C, aromatic	1.25	1.77
H	0.39	1.10
F	0.41	1.46

To obtain the electron densities, a MP2/6-31G** molecular-orbital calculation [23] was carried out for each molecule involved. Full geometry optimization was regarded as necessary for perfluorohexane because the assumption of a planar zigzag conformation was known to be incorrect. For the other molecules. the geometries found in the crystal structures were used without optimization, because minor geometry variations are unlikely to significantly alter the results. Point-charge parameters were obtained by the ESP procedure from the same calculation. This procedure derives point charges located at atomic nuclei that best fit the electrostatic potential generated by the molecular charge distribution.

Energy Partitioning. – Any partitioning of total interaction energies has a degree of arbitrariness, so that, in a sense, each method defines its own partitioned energies. Indeed, our partitioning is found to vary significantly for relatively small changes in the numerical value of the four disposable parameters. Only the electrostatic energies are parameter-free, and several checks show that they agree closely with values calculated by more sophisticated quantum-chemical methods. The PIXEL method, in its present formulation and parameterization, reproduces reasonably well the sublimation enthalpies of many organic crystals, as well as the interaction potential curves for some typical molecular dimers, both H-bonded and not, and yields reasonable trends concerning the relative importance of polar (electrostatic + polarization) *vs.* dispersive interaction energies among chemical classes [24]. Preliminary calculations show that the PIXEL partitioning compares well with intermolecular-perturbation-theory (IMPT) partitioning for nonpolar compounds. For polar and H-bonded compounds, PIXEL polarization energies are too large and dispersion energies too small. Furthermore, there are indications that the dependence of repulsion energy on overlap integral cannot be represented by a single proportionality constant; it appears, for example, that the constant should be larger for overlap between C⋯C densities and smaller for O⋯O densities. Our present parameterization is a reasonable compromise, but further adjustment is clearly needed. All these defects and discrepancies may be reduced by further manipulation of the parameters in the PIXEL method, and a systematic approach to adjusting these parameters for closer adherence to IMPT and experimental results is under way.

Comparison of PIXEL and UNI calculations. – The UNI force-field is of the simple form $E(r_{ij}) = A\ \exp(-Br_{ij}) - Cr_{ij}^{-6}$ where r_{ij} is the distance between any two atoms in different molecules. It goes back to the collection of A, B, C parameters given by *Gavezzotti* and *Filippini* several years ago [25]. Designed specifically for the organic solid state, this force field was calibrated against observed structures and sublimation

enthalpies of a collection of organic molecular crystals. A feature is that interaction parameters between different atom types are separately optimized, rather than assigned by averaging methods. A more-recent compilation, including F···F, C···F, and H···F interactions is available [26]. Although these potentials were developed in the UNI philosophy, *i.e.*, without explicit atom–atom point-charge electrostatic contributions, they may be supplemented with atom–atom coulombic contributions using ESP point charges placed at nuclear positions. This has been done in some of our dimer calculations in order to demonstrate differences between the PIXEL and the localized charge treatment of coulombic interactions. *Table 2* shows a preliminary comparison between the performance of the two methods, as well as the few available experimental data on sublimation enthalpies of fluoro compounds. Results of the calculations are shown in *Tables 3–6*, where stabilization energies are given as negative quantities.

Table 2. *Calculated Lattice Energies and Observed Heats of Sublimation for a Few Hydrocarbon and Fluorocarbon Crystals* (all energies in $kJ \cdot mol^{-1}$)

	ΔH(subl)	E(PIXEL)	E(UNI)[a])
1,1′-biphenyl	81.6	–	– 88.3
Perfluoro-1,1′-biphenyl	87.8		– 92.4
4,4′-Difluoro-1,1′-biphenyl	91.2		– 92.5
Benzene	44.4	– 47.7	– 44.4
Hexafluorobenzene	49.0	–	– 57.0
1,3,5-Trifluorobenzene	–		– 45.7
Naphthalene	72.3	– 69.5	– 72.8
Perfluoronaphthalene	79.5		– 80.7
Hexane	50.6	– 60.8	– 48.2
Perfluorohexane	–		– 64.0

[a]) UNI Energies in this table are calculated in the original formulation, without atom–atom point-charge electrostatic contributions

Aromatic Dimers. – For the aromatic dimers (*Table 3*), the energy minima were obtained for the face-to-face arrangements without lateral slip or rotation in the molecular plane. In the actual benzene/hexafluorobenzene co-crystal, adjacent molecules in the stacks are symmetry-independent; they are laterally displaced and mutually rotated. In the crystal structures of 1,3,5- and 1,2,3-trifluorobenzene, adjacent molecules in the stacks are related by inversion centers; they are thus antiparallel and laterally displaced. In our calculations, the energies of the dimers are found to change only little with such deviations from the face-to-face arrangement. For example, for the 1,3,5-trifluorobenzene dimer the change in PIXEL energy between the antiparallel face-to-face arrangement and corresponding arrangements displaced by 1 Å, at a fixed interplanar separation of 3.2 Å, is a destabilization of less than $1 kJ \cdot mol^{-1}$. A similar result is obtained from the UNI calculation. The observed stacking displacements in the actual crystal structures might well be due to the better interstack packing that can thereby be achieved.

Fig. 3 shows the energy curves for the interaction of the homo- and hetero-dimers of benzene and hexafluorobenzene. In all three cases, the energy well is relatively flat over

Table 3. *Interaction Energies* [kJ·mol^{-1}] *in Aromatic Dimers at the Equilibrium Inter-Ring Distance* [Å] *Estimated by Interpolation along the Energy Curves*[a])

		Distance	Ecoul	Epol	Edisp	Erep	Etot
(Benzene)$_2$	PIXEL	3.4	−0.8	−4.0	−32.3	23.5	−13.6
	UNI	3.6	+6.3	–	−27.2	10.7	−10.2
(Benzene-HFBZ)	PIXEL	3.2	−22.5	−10.9	−45.5	45.9	−33.1
	UNI	3.5	−6.6	–	−35.6	15.8	−26.3
(HFBZ)$_2$	PIXEL	3.2	−6.4	−10.0	−48.8	42.1	−22.8
	UNI	3.5	7.9	–	−41.0	16.9	−16.2
(1,3,5-TFB)$_2$, parallel	PIXEL	3.3	−7.4	−3.7	−39.6	32.3	−18.4
	UNI	3.5	1.5	–	−35.8	15.8	−18.4
(1,3,5-TFB)$_2$, antiparallel	PIXEL	3.2	−18.6	−7.5	−46.0	46.0	−26.2
	UNI	3.5	−1.4	–	−35.6	15.8	−21.2
(1,2,3-TFB)$_2$, parallel	PIXEL	3.4	−2.3	−2.5	−34.2	21.8	−17.2
	UNI	3.6	+4.2	–	−30.9	11.2	−15.6
(1,2,3-TFB)$_2$, antiparallel	PIXEL	3.2	−20.3	−7.8	−46.0	47.8	−26.2
	UNI	3.5	−4.5	–	−35.2	15.6	−24.1

[a]) For the UNI results, Ecoul denotes the atom-atom point-charge electrostatic term over ESP charges, Edisp denotes the R^{-6} attractive part of the potential, and Erep denotes the exp(−R) repulsive part. Total UNI energies include the Ecoul contribution.

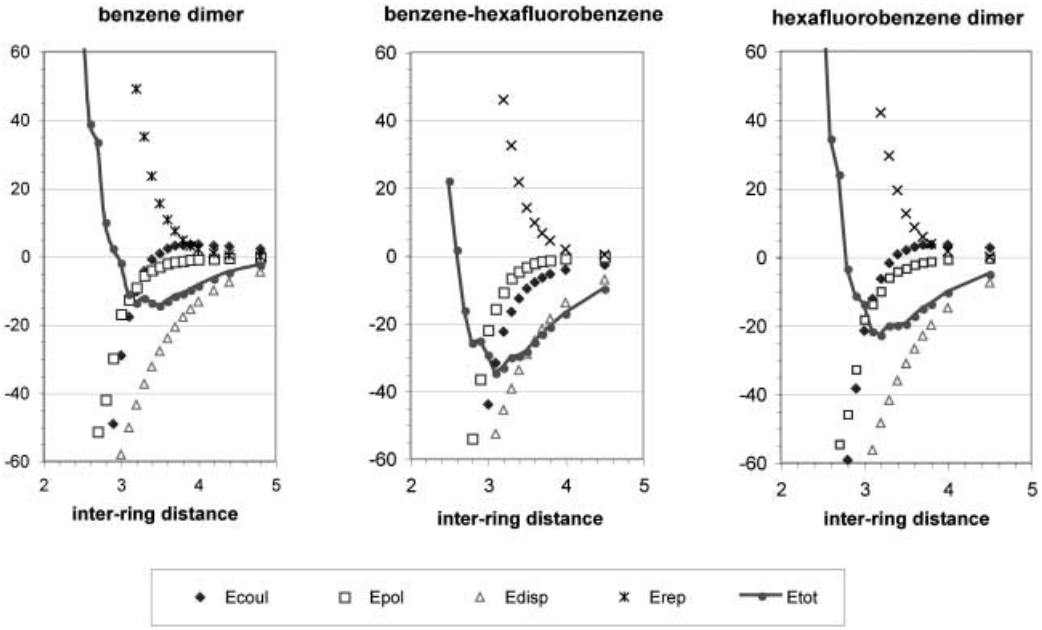

Fig. 3. *Plots of energy* vs. *inter-ring distance for benzene and hexafluorobenzene homo- and hetero-dimers, as obtained by the PIXEL method.* The solid curves connect total energy points.

a range of 0.3–0.5 Å, with small fluctuations that are intrinsic to the numerical accuracy of the method, as discussed previously [24], so that the exact location of the minimum is somewhat imprecise. The coulombic energies show a similar trend in the

homo-dimers. They are slightly destabilizing at long distances and become stabilizing at short distances. In the hetero-dimer, the coulombic contribution is stabilizing throughout, and it is clearly this contribution that makes the hetero-dimer more stable than the homo-dimers. In all cases, however, it is dispersion that makes the largest contribution to the net stabilization. In comparison with experimental inter-ring distances in crystals (3.5 to 3.7 Å), the PIXEL equilibrium distances are too short; the UNI distances are closer to experiment (*Table 3*). Incidentally, we have calculated the energies of stacked trimers, and found them to be twice as large as those of the dimers. Thus, according to our calculations, interactions between nearest neighbors in the stacks contribute a negligible amount to cohesive energies.

Table 3 also shows the energies at the minima found in the potential-energy curves. The PIXEL energy changes from $-14\ kJ\cdot mol^{-1}$ (at 3.4 Å) for benzene dimer to $-23\ kJ\cdot mol^{-1}$ for hexafluorobenzene dimer (at 3.2 Å), to $-33\ kJ\cdot mol^{-1}$ (at 3.2 Å) for the hetero-dimer. For 1,3,5-trifluorobenzene the dimer energy is $-18\ kJ\cdot mol^{-1}$ for the parallel and $-26.2\ kJ\cdot mol^{-1}$ for the anti-parallel arrangement, while for the 1,2,3-isomer the corresponding energies are $-17\ kJ\cdot mol^{-1}$ (at 3.4 Å) and $-26\ kJ\cdot mol^{-1}$ (at 3.2 Å). Remarkably, the UNI energies follow a quite similar trend. In comparison with results obtained by high-level quantum-chemical calculations for aromatic dimers, the PIXEL binding energies are too large and the equilibrium distances too short: thus, for the benzene dimer, CSSD (T) (Coupled Cluster Single, Double and Triple excitations; a form of highly correlated quantum-chemical calculation) results [27] are $-4\ kJ\cdot mol^{-1}$ and 4.1 Å compared with $-13.6\ kJ\cdot mol^{-1}$ and 3.4 Å. Whereas the PIXEL distance seems slightly too short, the CSSD(T) distance seems too large. Indeed, if PIXEL energy results are sensitive to numerical accuracy and to small changes in parameterization, quantum-chemical calculations also give quite a spread, depending on the choice of method, basis set, and basis-set superposition treatment, and other subtle factors, particularly where the energy of interest results from the tiny imbalance between huge positive and negative energy values.

The relative importance of the various energy contributions in the aromatic dimers is perhaps better appreciated from a comparison at a constant inter-ring distance of 3.4 Å (*Table 4*). At this distance, the dimer energy is $-14\ kJ\cdot mol^{-1}$ for benzene, $-20\ kJ\cdot mol^{-1}$ for hexafluorobenzene, -17 to $-25\ kJ\cdot mol^{-1}$ for the trifluorobenzenes, and $-30\ kJ\cdot mol^{-1}$ for the hexafluorobenzene-benzene hetero-dimer. The corresponding UNI energies are within 3 to 5 $kJ\cdot mol^{-1}$ of these values, with one striking exception. This is 1,2,3-trifluorobenzene, for which the UNI force field gives an energy of only -2

Table 4. *PIXEL Interaction Energies* [$kJ\cdot mol^{-1}$] *in Aromatic Dimers at a Fixed Inter-Ring Distance of 3.4 Å*

	Ecoul	Epol	Edisp	Erep	Etot
$(Benzene)_2$	– 0.8	– 4.0	– 32.3	23.5	– 13.6
(BZ-HFBZ)	– 12.7	– 4.7	– 33.8	21.6	– 29.7
$(HFBZ)_2$	– 0.8	– 4.2	– 36.0	19.4	– 19.9
$(1,3,5\text{-TFB})_2$, parallel	– 4.1	– 2.3	– 34.2	21.5	– 19.0
$(1,3,5\text{-TFB})_2$, antiparallel	– 8.4	– 2.4	– 34.2	22.5	– 24.9
$(1,2,3\text{-TFB})_2$, parallel	– 2.3	– 2.5	– 34.2	21.8	– 17.2
$(1,2,3\text{-TFB})_2$, antiparallel	– 10.3	– 2.9	– 34.2	22.5	– 24.9

to $-3\ kJ \cdot mol^{-1}$ for the parallel arrangement. The reason is found to lie in the unrealistic electrostatic contribution of *ca.* $+20\ kJ \cdot mol^{-1}$ arising from the localized point charges placed at the atomic nuclei. These charges were obtained by optimal fitting to the electrostatic potential due to the charge density based on the Gaussian calculation, so the discrepancy arises not from incorrect assignment of charges but from the inadequacy of the localized point-charge model at such short intermolecular distances.

As is clear from *Table 4*, the dispersion energy makes the main contribution to the total energy. It increases slightly from benzene through the trifluorobenzenes to hexafluorobenzene. This trend runs parallel to the change in ionization potential, the *E*(HOMO) increasing from 0.330 to 0.360 to 0.377 eV in the same sequence. Interestingly, the overlap repulsion decreases along the same sequence, a further confirmation of the contraction of the charge density in fluorinated hydrocarbons. These variations are, however, at the borderline of significance, given the possible influence of many other electronic and geometrical factors. Polarization energies are also fairly constant in all the 3.4-Å aromatic dimers. The only energy term with a clearly significant difference is the coulombic energy, which is close to zero for the benzene and hexafluorobenzene homo-dimers and $-12.7\ kJ \cdot mol^{-1}$ for the benzene-hexafluorobenzene hetero-dimer. For 1,3,5-trifluorobenzene, the parallel and anti-parallel dimer arrangements have a coulombic energy of -4 and $-8\ kJ \cdot mol^{-1}$ respectively, while for 1,2,3-trifluorobenzene the coulombic energy of the antiparallel configuration is markedly larger than that of the parallel one, -10 *vs.* $-2\ kJ \cdot mol^{-1}$. Note that these coulombic energies are all stabilizing, even if they are small. The contrast with the $+20\ kJ \cdot mol^{-1}$ coulombic-repulsion energy estimated for the 1,2,3-triflurobenzene homo-dimer with the localized-charge model could not be greater.

On the whole, our calculations predict a stabilization of all dimers where F-atoms and H-atoms are juxtaposed, more or less as expected from elementary electrostatic arguments. The main difference between the PIXEL and UNI results is that the former consistently predict a larger energy separation between the staggered and eclipsed configurations of the 1,3,5-trifluorobenzene dimer. The description of coulombic energies by the PIXEL procedure differs substantially from the localized point charge scheme in UNI. It can hardly be expected that a simple model based on a dozen point charges per molecule can perform as well as one that approximates the actual charge distribution by a grid containing about a thousand times as many points. The PIXEL procedure is more rigorous and includes penetration energies.

If coulombic energies obtained with the point-charge model at short intermolecular distances are unreliable, what are we to say about energies estimated from electric quadrupole-moment calculations? The quadrupole moments of benzene and hexafluorobenzene are large and of opposite sign ($-29 \times 10^{-40}\ C\ m^2$ for benzene, $+32 \times 10^{-40}\ C\ m^2$ for hexafluorobenzene), and far-reaching conclusions about interactions between these molecules have been drawn from this [28]. More generally, the role of molecular quadrupole–quadrupole interactions between benzene rings and their fluorinated counterparts has been invoked as an important factor in stabilizing mixed stacks involving such systems. Indeed, the quadrupole–quadrupole model has the advantage of simplicity – but little else. It is quite useless in estimating even rough values of the stabilization energies of molecular dimers. The interaction energy of two

quadrupoles θ_B and θ_B at distance R is given by $N\theta_A\theta_B/4\pi\varepsilon_0 R^5$ where N is a numerical factor that depends in a fairly complicated way on the mutual orientation of the two quadrupoles [29]. For two quadrupoles with equal sign oriented as in the face-to-face benzene or hexafluorobenzene homo-dimers, N has the value $+6$; with quadrupoles of opposite sign oriented as in the benzene-hexafluorobenzene hetero-dimer, N has the value -6. With both quadrupole moments assigned a magnitude of 30×10^{-40} C m^2 and $R = 3.6$ Å, the interaction energy becomes ± 48 kJ · mol^{-1}, with positive sign for the homo-dimers and negative sign for the hetero-dimer. These values are quite unrealistic and have no relation to the coulombic energies calculated by the PIXEL method. As noted by *Fowler* and *Buckingham* [30], the use of point multipoles to estimate molecular interaction energies at distances that are comparable to (or less than) the molecular sizes is 'prone to error'. It cannot be expected to produce meaningful results.

Lateral Interactions between Aromatic Rings. – We have performed calculations on the lateral interactions between two benzene or two 1,3,5-trifluorobenzene molecules in the centrosymmetric arrangement shown in *Fig. 4*, by varying systematically the distance between the ring centroids. As noted by *Thalladi et al.* [15], this motif is observed in the crystal structure of 1,3,5-trifluorobenzene with F···H distance of 2.45 Å. *Table 5* shows the agreement between calculated and observed H···F distances. As judged from the energy partitioning, the trifluorobenzene system, as compared with the hydrocarbon counterpart, experiences a small coulombic stabilization between electron-rich F and electron-deficient H regions. Both PIXEL and UNI calculations describe this lateral interaction as very weak. In particular, the difference between the benzene pair and the trifluorobenzene pair is 2.2 (PIXEL) or 3.8 (UNI) kJ · mol^{-1}, so that if this difference is attributed entirely to the two C–H···F interactions the energy of a single such C–H···F 'H-bond' can be estimated as 1–2 kJ · mol^{-1}. The stacking energy in the antiparallel dimer is many times greater.

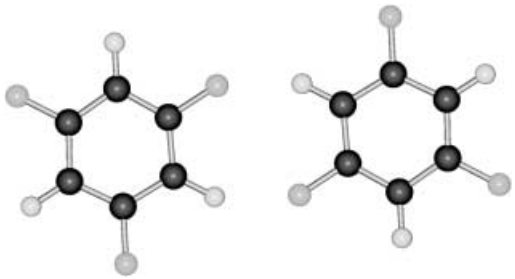

Fig. 4. *Centrosymmetric pair of 1,3,5-trifluorobenzene molecules, as observed in the crystal structure* [15]

Table 5. *Interaction Energies* [kJ · mol^{-1}] *between Aromatic Rings as in* Fig. 3

		R [Å]	Ecoul	Epol	Edisp	Erep	Etot
1,3,5-TFB	PIXEL	2.6 (H···F)	–4.5	–0.7	–3.5	4.2	–4.5
	UNI	2.6 (H···F)	–3.0	–	–6.3	3.6	–5.7
Benzene	PIXEL	2.4 (H···H)	0.4	–0.8	–5.0	3.0	–2.3
	UNI	2.6 (H···H)	0.8	–	–4.4	1.7	–1.9

Aliphatic Dimers. – A preliminary set of calculations was performed for dimers of methane and of tetrafluoromethane, by varying the distance between the respective C-atoms and keeping two C–H or C–F bonds colinear, in the arrangement $X_3C-X\cdots X_3C-X$ (X = H or F). Results are shown in *Table 6*. The PIXEL interaction energy is larger than the UNI energy for the methane dimer and smaller for the tetrafluoromethane dimer; correspondingly, the PIXEL equilibrium distance is shorter for the methane dimer and longer for the tetrafluoromethane dimer. We note that, for the methane dimer, PIXEL gives an equilibrium geometry in which the two molecules are in *Van der Waals* contact, the C···H distance of 2.80 Å being just less than the sum of intermolecular radii (see *Table 1*), while UNI gives a looser contact. The well-depth for the $CH_4\cdots CH_4$ interaction has been estimated to lie in the range 1.5–2.5 kJ·mol^{-1}[30], compared with which the PIXEL energy is slightly too high and the UNI energy too low. For the tetrafluoromethane dimer, the equilibrium distances obtained by the two methods are identical and close to the sum of *Van der Waals* radii, but PIXEL gives a smaller interaction energy.

Table 6. *Equilibrium Distances* [Å] *and Interaction Energies* [kJ·mol^{-1}] *in Dimers of Methane and Tetrafluoromethane*

Dimers	Distance			Ecoul	Epol	Edisp	Erep	Etot	
		PIXEL	UNI	PIXEL	PIXEL	PIXEL	PIXEL	PIXEL	UNI
$H_3C-H\cdots H_3C-H$	C···H	2.80	3.20	−1.4	−0.5	−5.1	3.9	−3.2	−1.2
$F_3C-F\cdots F_3C-F$	C···F	3.27	3.27	−0.1	−0.1	−2.9	0.9	−2.1	−2.8

The hexane and perfluorohexane homo-dimers, together with the mixed hetero-dimer were then considered. The potential-energy surfaces are here more complicated than for the stacked aromatic dimers. The hexane system with its planar zigzag chain is the easiest to describe. We choose the *x*-axis along the chain, the *y*-axis in the plane of the C-atoms, and the *z*-axis perpendicular to this plane. With the first molecule at the origin of coordinates, the second molecule is placed at *x*, *y*, *z* and may also be rotated through an angle φ about the chain direction. For perfluorohexane, we take the same system, except that the *y*-axis is now in the mean plane of the C-atoms rather in the exact plane. The energy surface was then explored by systematically changing these parameters. We are fairly confident that the introduction of other degrees of freedom would give only marginally different results.

Figs. 5 and *6* look almost identical but they show small differences and are derived from completely disparate and independent bases. *Fig. 5* is based solely on the results of our calculations for hexane and perfluorohexane; H1 and H2 depict the two dimers with the lowest calculated energy for hexane, and P1 and P2 provide the same information for perfluorohexane (*Table 7*). *Fig. 6* is based on the crystal structures of the two compounds. Here H1 and H2 show the arrangement of successive molecules along the two shortest translations of the hexane crystal [9], and P1 and P2 show corresponding arrangements in the perfluorohexane crystal [10]. In the latter case the P2 pair are not related by pure translation but by glide-reflection; the two molecules in the pair have opposite sense of chirality. The agreement between the calculated pairs and the observed arrangements in the crystal structures could not be better.

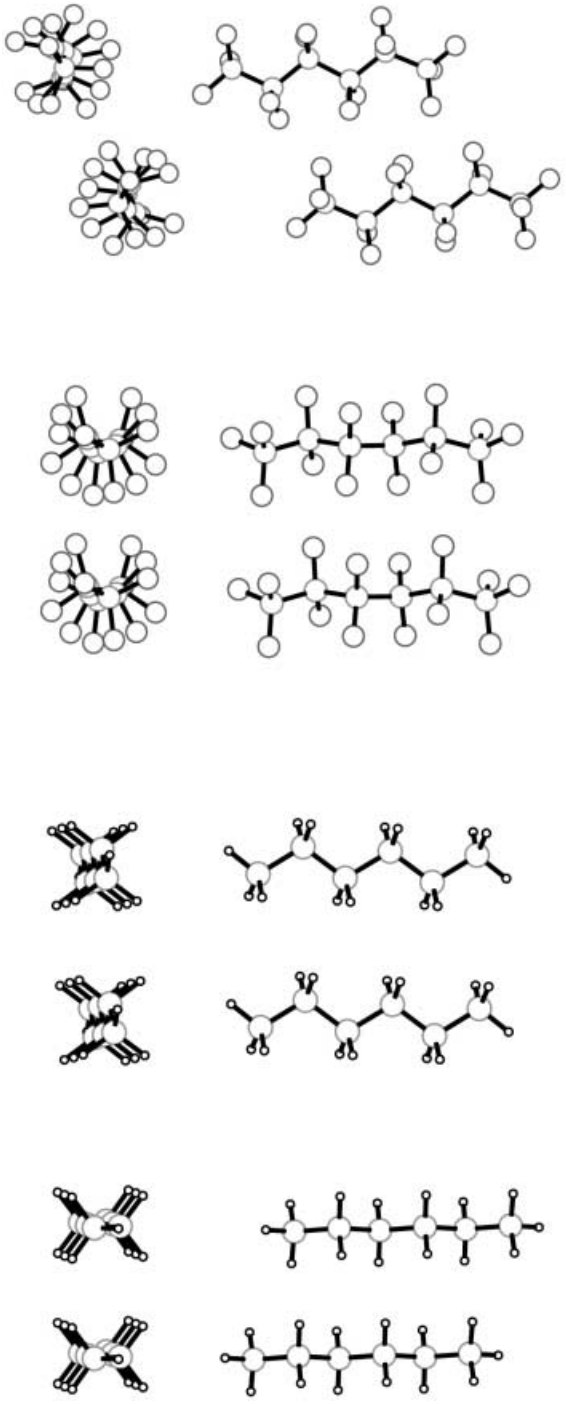

Fig. 5. *Minimum-energy arrangements of hexane and perfluorohexane homo-dimers, as calculated by the PIXEL method* (see *Table 6*). The hexane dimers H1 and H2 are closely similar to dimers formed by successive molecules related by translation in the hexane crystal structure [10]. The perfluorohexane dimers P1 and P2 are similar to those formed by successive molecules related by translation (P1) and glide-reflection (P2) in the perfluorohexane crystal [11] (see text and *Fig. 6*).

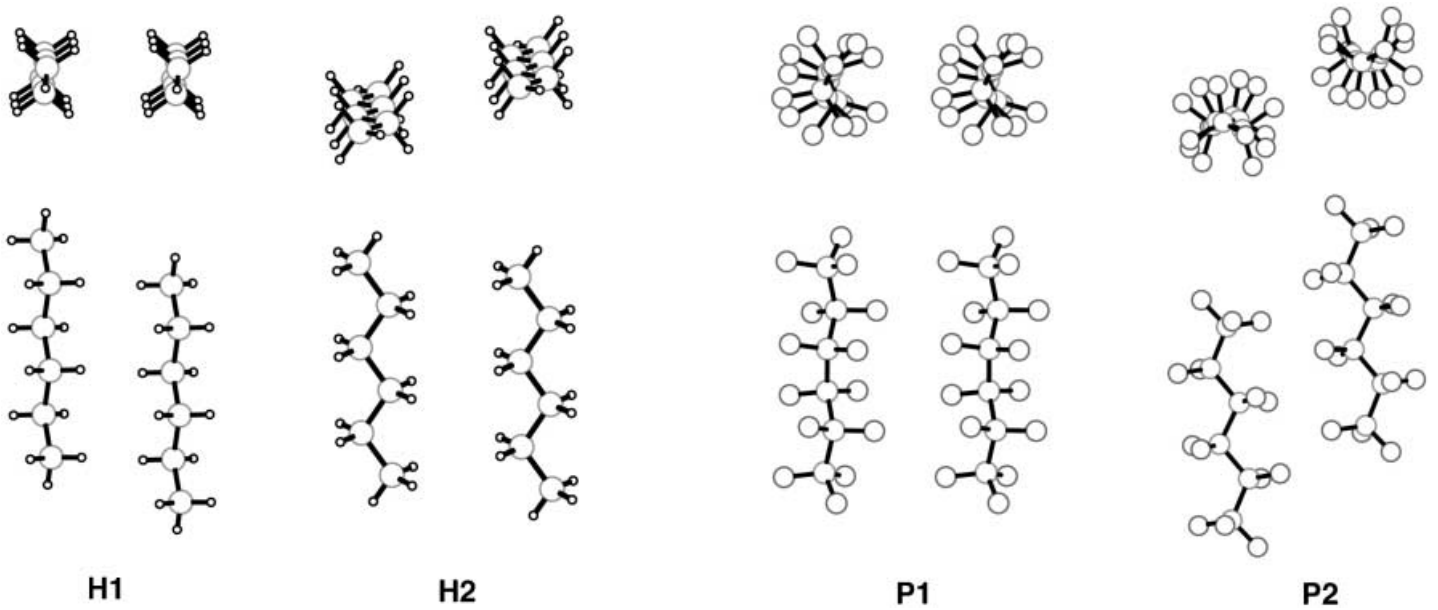

Fig. 6. *Crystal structures. H1 and H2:* Patterns of successive molecules related by translation along the short cell axes $c = 4.13$ Å and $b = 4.97$ Å in the crystal structure of hexane [10]. *P1 and P2:* Patterns of successive molecules related by translation along the shortest cell axis $b = 5.15$ Å and by glide-reflection (center-to-center distance 5.87 Å) in the crystal structure of perfluorohexane [11]. Compare with the corresponding calculated dimer structures in *Fig. 5*.

Table 7. *Equilibrium Distances* [Å] *and Interaction Energies* [kJ·mol^{-1}] *in Low-Energy Hexane and Perfluorohexane Homo-Dimers.* See *Fig. 5* and compare with *Fig. 6*.

Dimer	Distance		Ecoul		Epol	Edisp		Erep		Etot	
	PIXEL	UNI	PIXEL	UNI		PIXEL	UNI	PIXEL	UNI	PIXEL	UNI
H1 $(Hexane)_2$	3.8	4.1	−8.5	+0.7	−3.8	−37.4	−23.4	27.8	25.7	−22.0	−13.6
H2 $(Hexane)_2$	4.4	4.6	−5.1	0.0	−2.1	−27.1	−19.0	17.3	7.2	−17.0	−11.8
P1 $(Perfluorohexane)_2$	5.1	4.9	−0.8	−0.4	−0.1	−12.2	−24.1	3.9	6.5	−9.1	−18.6
P2 $(Perfluorohexane)_2$	6.0	5.8	−0.3	−0.1	0.0	−9.6	−22.2	2.4	4.4	−7.6	−15.3

As far as the energies are concerned, the PIXEL and UNI methods yield discordant results. For the hexane dimers H1 and H2, PIXEL gives a greater stabilization energy than UNI (−22.0 *vs.* −13.6 kJ·mol^{-1}for H1, −16.7 *vs.* −11.6 kJ·mol^{-1}for H2), whereas, for the perfluorohexane dimer, it is the other way round (−9.1 *vs.* −18.6 kJ·mol^{-1}for P1, −7.6 *vs.* −14.4 kJ·mol^{-1}for P2). In other words, the increase in intermolecular distance on going from the hexane dimers to the perfluorohexane dimers is associated with a decrease in binding energy according to the PIXEL calculation but with an increase according to the UNI calculation. This difference depends mainly on the manner in which the dispersion and repulsion energies vary with distance in the two kinds of calculation. Note also that in the PIXEL calculations, the coulombic contribution to the binding energy of the hexane dimers is significant, whereas it is negligible for the perfluorohexane dimers at considerable greater separation. In the UNI calculation the coulombic energy is negligible for both sets of dimers. It is possible that, as far as the net energies of the hexane dimers are concerned, the UNI result may be more realistic, since the total lattice energy of the hexane crystal is overestimated by PIXEL and reasonably well approximated by UNI (see *Table 2*).

Turning now to the hexane-perfluorohexane system, the low-energy dimer HP1 (*Table 8* and *Fig. 7*) is somewhat similar to the best perfluorohexane dimer P1 (*Table 6* and *Fig. 7*), but here there is no experimental structure for comparison. The same lack applies to the other calculated low-energy dimers HP2 and HP3. Although the pattern of energies is different for the PIXEL and UNI calculations, they agree that the binding energy of the hetero-dimer is not greater than that of the homo-dimers but less – in sharp contrast to the results for the aromatic dimers.

Discussion. – We have described in this paper some calculations on prototypical dimers involving hydrocarbon molecules and their fluorinated counterparts, as well as some calculations of lattice energies of fluorinated compounds, using a newly

Table 8. *Equilibrium Distances* [Å] *and Interaction Energies* [kJ·mol^{-1}] *in Low-Energy Hetero-Dimers.* See *Fig. 7*.

Dimer	Distance		Ecoul		Epol	Edisp		Erep		Etot	
	PIXEL	UNI	PIXEL	UNI		PIXEL	UNI	PIXEL	UNI	PIXEL	UNI
HP1	4.9	4.9	−1.0	0.0	−0.4	−11.9	−16.9	4.7	4.0	−8.5	−12.9
HP2	5.0	5.0	−1.1	−0.1	−0.4	−10.4	−15.2	5.1	3.8	−7.0	−11.3
HP3	5.0	5.0	−1.1	0.0	−0.4	−11.9	−16.9	5.4	4.3	−8.0	−12.6

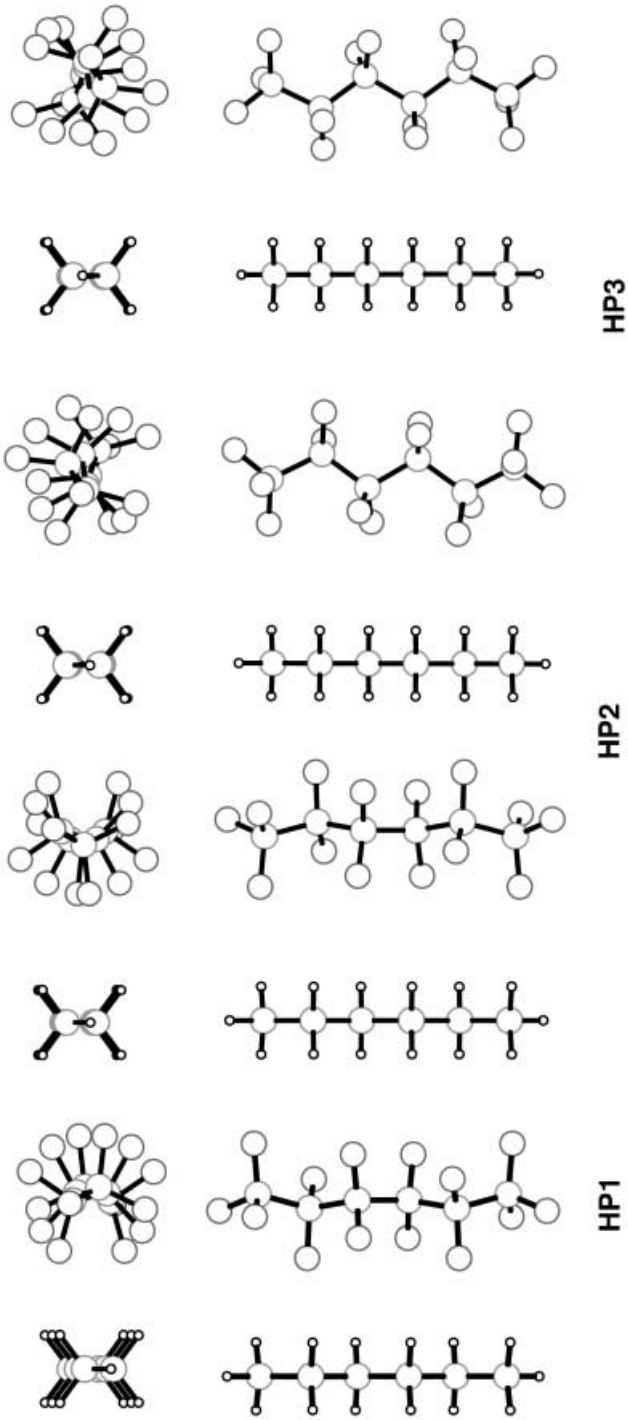

Fig. 7. *Three representative low-energy pairs HP1, HP2, HP3* (*Table 8*) *calculated for the hexane-perfluorohexane hetero-dimer*. No crystal structure is available for comparison.

developed semi-classical method, PIXEL, and standard force-field atom–atom potentials. Significantly, the PIXEL results are much more informative than the atom-atom ones, for only a modest increase of the computing effort. In particular, the detailed discussion of some of the dimerization energies shows that PIXEL is not doing so much worse than high-level, elaborate, and computationally demanding quantum-chemical methods. We take these results as further encouragement to pursue the optimization of the PIXEL procedure until a few existing malfunctions, notably in the calculation of overlap repulsion energies, may be repaired.

So where has all this gotten us? The relatively simple models followed in this study seem to provide some intuitive insight into the problem of hydrocarbon-fluorocarbon compatibility. In the aromatic series, PIXEL and UNI calculations agree that the binding energy of the benzene-hexafluorobenzene dimer is markedly greater than the energies of the corresponding homo-dimers. In the aliphatic series, the binding energy of the hexane-perfluorohexane dimer is less than the energies of the corresponding homo-dimers. This is in accord with the contrasting behavior of aromatic and aliphatic hydrocarbon/fluorocarbon mixtures, as outlined in the *Introduction*. While we may be pleased by this outcome, we are well aware that we are still far from a proper theoretical explanation of the behavior of the real systems. We therefore refrain from making any inferences about thermodynamic aspects of these systems, such as internal energies of liquid or solid phases, on the basis of our oversimplified dimer models. However, an analysis of the energy dissection afforded by PIXEL seems to provide some general relationships between molecular shape and intermolecular interaction energies of aliphatic and aromatic systems.

Dispersion seems to be by far the most-important cohesive contribution, at least in magnitude, if not in directionality. Contacts between C-atoms are much more effective than contacts between F-atoms, because of the large difference in atomic polarizability (see *Table 1*). The difference between aliphatics and aromatics seems to be mainly a matter of the difference in molecular shape. In the aromatic dimers, the disk shape of the molecules with H-atoms on the rim allows C-atoms of the separate molecules to maintain a close distance of *ca.* 3.4 Å, and hence to provide a substantial and nearly constant dispersion energy throughout the series. The coulombic energy of the hetero-dimer then plays the decisive contribution to its greater stability over the homo-dimers. The same is true, to only a slightly lesser extent, for the 1,2,3- and 1,3,5-trifluorobenzene dimers in suitable mutual orientation.

In the aliphatic series, C-atoms are less polarizable in the first place (*Table 1*; recall that dispersion energy goes as the *product* of the polarizabilites), and the planar zigzag or helical-chain molecular shape has them buried in the internal part of the molecule and hence more shielded from external influence, so the story is quite different. The closest intermolecular C···C distances in the hexane homo-dimer are only slightly greater than those in the aromatic dimers, because the C-atoms are interspaced by comparatively small H-atoms, but the F-atoms in the perfluorohexane molecule with their larger packing radius get in the way of any close contact between C-atoms of different molecules (the molecular volume of perfluorohexane is 210 $Å^3$ compared with 136 $Å^3$ for hexane itself). Hence, dispersion energies are much smaller. In addition, there is little gain in coulombic energy in the aliphatic hetero-dimer, so the net result is indifference or even destabilization upon mixing.

For hexane and perfluorohexane, the agreement between the best calculated homodimers and the pairs formed by successive molecules in the crystal structures (*Figs. 5* and *6*) is an unexpected bonus. Both crystal structures are built from layers of parallel molecules in which the two basic molecule-to-molecule alignments correspond very closely to the best pairings obtained in our calculations. In the hexane crystal, the space group $P\bar{1}$ with $Z = 1$ ensures exact parallelism of the centrosymmetric molecules; in the perfluorohexane crystal (space group $I2/a$, $Z = 8$) the parallelism of enantiomeric molecules related by the glide-plane is not enforced by symmetry but is a result of the packing. In essence, we have come close to predicting (or rather post-dicting) the two crystal structures without setting out to do so. All that remains would be to find the optimal interlayer arrangement of terminal Me (or CF_3) groups, and there are not many possibilities.

We cannot claim a corresponding success in the aromatic series. Crystal structures are available for 1,2,3- [10] and 1,3,5-trifluorobenzene [15] and for the benzene/hexafluorobenzene co-crystal [18]. In none of these does the calculated dimer correspond very closely to the arrangements found in the crystal stacks. As mentioned earlier, the crystal structures show lateral displacements or rotations of successive molecules in the stacks, whereas our calculated dimers have their minimum energy for face-to-face structures without lateral slip or rotation (although the energy wells were rather flat in almost all cases). It is quite possible that the observed deviations between the slipped stacks in the crystal and the perfect face-to-face arrangement in the dimers result from the improved interstack packing that could thereby be achieved. For the packing of two-dimensional layers in the aliphatic series, any loss of packing energy in distorting the layers would be less likely to be compensated by improved inter-layer packing of terminal methyl (or trifluoromethyl) groups.

The relatively large value of the coulombic energy for the stable hexane dimer according to the PIXEL calculation ($-8.6\ kJ \cdot mol^{-1}$, *Table 7*) may come as a surprise in view of the usual description of interactions among such aliphatic hydrocarbons as 'nonpolar'. Indeed, this coulombic contribution to the stabilization energy is comparable to, even slightly larger than, the corresponding term calculated for the T-shaped benzene dimer ($-6.4\ kJ \cdot mol^{-1}$). This T-shaped dimer is traditionally regarded as the prototype of a $C-H\cdots\pi$ interaction or alternatively as the expression of the interaction between two electric quadrupole moments of like polarity. If either of these models is accepted, what are we then to say about the origin of the substantial coulombic attraction between the H1 pair of parallel hexane molecules as shown in *Fig. 6*?

We are grateful to Prof. *Roland Boese* for determining the crystal structure of 1,2,3-trifluorobenzene at our request and for providing information about it and about the unpublished crystal structure of perfluorohexane.

REFERENCES

[1] J. H. Hildebrand, J. M. Prausnitz, R. L. Scott, 'Regular and Related Solutions', Van Nostrand Reinhold, New York, 1970.
[2] E. M. Dantzler Siebert, C. M. Knobler, *J. Phys. Chem.* **1971**, *75*, 3863.
[3] C. R. Patrick, G. S. Prosser, *Nature* **1960**, *187*, 1021.
[4] A. Gavezzotti, *J. Phys. Chem., B* **2002**, *106*, 4145.
[5] A. Gavezzotti, *J. Phys. Chem., B* **2003**, *107*, 2344.

[6] P. T. van Duijen, M. Swart, *J. Phys. Chem., A* **1998**, *102*, 2399.
[7] J. F. Liebman, in 'Fluorine-Containing Molecules: Structure, Reactivity and Applications' Eds. J. F. Liebman, A. Greenberg, W. R. Dolber, VCH, Weinhem, 1988, p. 317ff.
[8] B. E. Smart, in 'Chemistry of Organic Fluorine Compounds', Eds. M. Hudlicky, A. E. Parlath, ACS Monograph 187, ACS, Washington DC, p. 979ff.
[9] B. E. Smart, *J. Fluorine Chem.* **2001**, *109*, 3.
[10] R. Boese, H.-C. Weiss, D. Bläser, *Angew. Chem.*, *Int. Ed.* **1999**, *38*, 988.
[11] R. Boese (Universität Essen), personal communication, 2003
[12] C. W. Bunn, E. R. Howells, *Nature (London)* **1954**, *174*, 549.
[13] E. S. Clark, L. T. Muus, *Acta Crystallogr.* **1960**, *13*, 1104.
[14] J. Lapasset, J. Moret, M. Melas, A. Collet, M. Vigeur, H. Blancou, *Z. Kristallogr.* **1996**, *211*, 945.
[15] V. R. Thalladi, H.-C. Weiss, D. Bläser, R. Boese, A. Nangia, G. R. Desiraju, *J. Am. Chem. Soc.* **1998**, *120*, 8702.
[16] B. P. van Eijck, A. L. Spek, W. T. M. Mooij, J. Kroon, *Acta Crystallogr.*, *Sect. B* **1998**, *54*, 291.
[17] G. J. Jeffrey, J. R. Ruble, R. K. McMullan, J. A. Pople, *Proc. R. Soc. London, Ser. A* **1987**, *414*, 47.
[18] J. W. Williams, J. K. Cockcroft, A. N. Fitch, *Angew. Chem.*, *Int. Ed.* **1992**, *31*, 1655.
[19] M. R. Battaglia, A. D. Buckingham, J. H. Williams, *Chem. Phys. Lett.* **1981**, *79*, 421.
[20] J. Vrbancich, G. L. D. Ritchie, *J. Chem. Soc.*, *Faraday Trans.* **1980**, *76*, 648.
[21] N. Boden, P. P. Davis, C. H. Stam, G. A. Wesselink, *Mol. Phys.* **1973**, *81*, 81.
[22] R. Boese, T. Clark, A. Gavezzotti, *Helv. Chim. Acta* **2003**, *86*, 1085.
[23] M. J. Frisch, G. W. Trucks, H. B. Schlegel, G. E. Scuseria, M. A. Robb, J. R. Cheeseman, V. G. Zakrzewski, J. A. Montgomery Jr., R. E. Stratmann, J. C. Burant, S. Dapprich, J. M. Millam, A. D. Daniels, K. N. Kudin, M. C. Strain, O. Farkas, J. Tomasi, V. Barone, M. Cossi, R. Cammi, B. Mennucci, C. Pomelli, C. Adamo, S. Clifford, J. Ochterski, G. A. Petersson, P. Y. Ayala, Q. Cui, K. Morokuma, P. Salvador, J. J. Dannenberg, D. K. Malick, A. D. Rabuck, K. Raghavachari, J. B. Foresman, J. Cioslowski, J. V. Ortiz, A. G. Baboul, B. B. Stefanov, G. Liu, A. Liashenko, P. Piskorz, I. Komaromi, R. Gomperts, R. L. Martin, D. J. Fox, T. Keith, M. A. Al-Laham, C. Y. Peng, A. Nanayakkara, M. Challacombe, P. M. W. Gill, B. Johnson, W. Chen, M. W. Wong, J. L. Andres, C. Gonzalez, M. Head-Gordon, E. S. Replogle, and J. A. Pople, *Gaussian 98*, Revision A.11, *Gaussian*, *Inc.*, Pittsburgh PA, 2001.
[24] A. Gavezzotti, *Cryst. Eng. Commun.* **2003**, *5*, 429.
[25] A. Gavezzotti, G. Filippini, *J. Phys. Chem.* **1994**, *98*, 4831.
[26] A. Gavezzotti, in 'Theoretical Aspects and Computer Modeling of the Molecular Solid State', Ed. A. Gavezzotti, John Wiley, Chichester, 1997, p. 67.
[27] P. Hobza. H. L. Selzle, E. W. Schlag, *J. Phys. Chem.* **1996**, *100*, 18790.
[28] J. H. Williams, *Acc. Chem. Res.* **1993**, *26*, 593.
[29] A. J. Stone, 'The Theory of Intermolecular Forces', Clarendon Press, Oxford 1996, p. 3.
[30] P. W. Fowler. A. D. Buckingham. *Chem. Phys. Lett.* **1991**, *176*, 11.

Received September 23, 2003